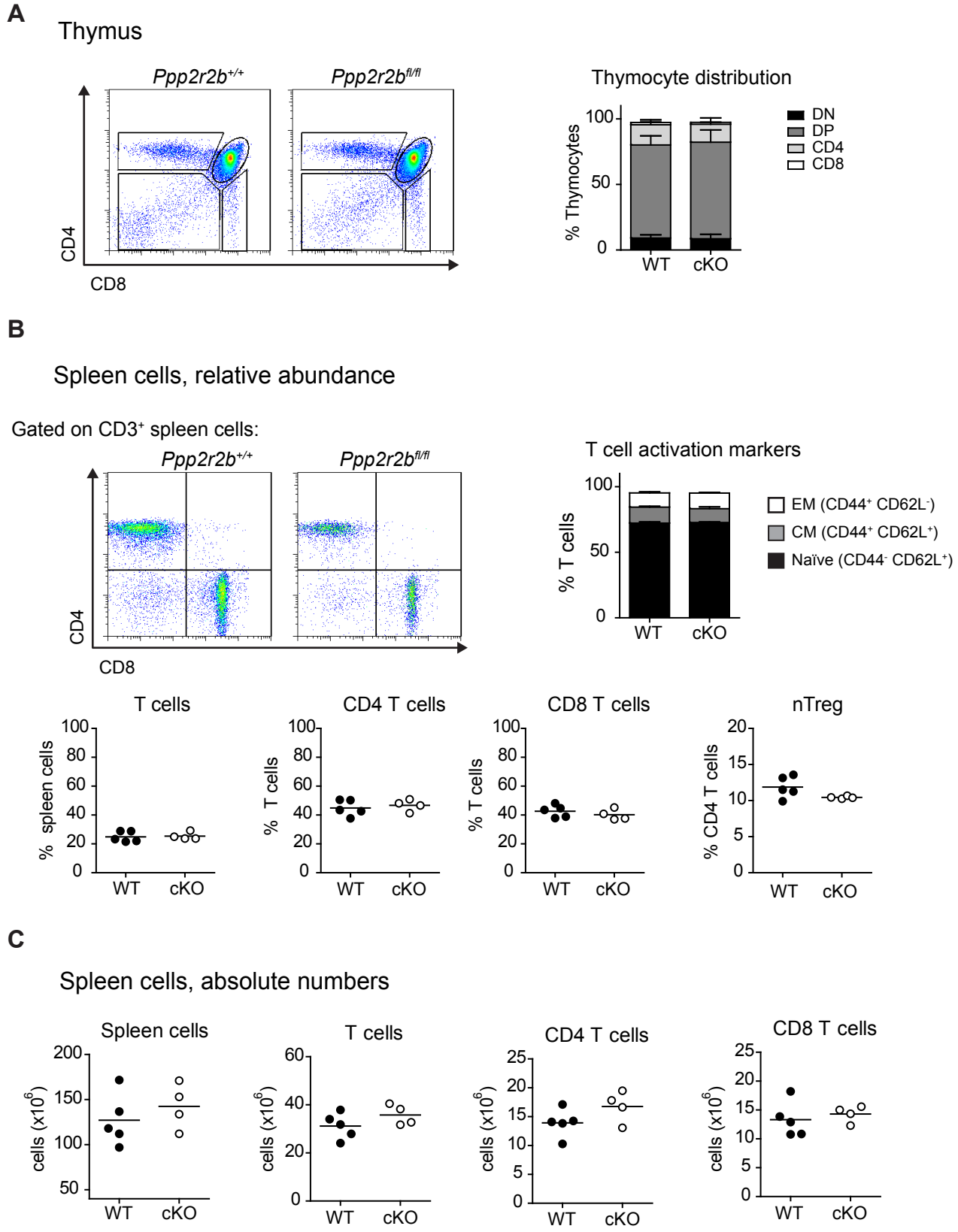

Supplemental Figure 1. The development of the immune system is normal in *Ppp2r2b* conditional knockout (cKO) mice. (**A**) Thymi of 6-week-old wild-type (WT; *Ppp2r2b*$^{+/+}$*Cd4*.Cre^{+}) and cKO (*Ppp2r2b*$^{fl/fl}$*Cd4*.Cre^{+}) were analyzed by flow cytometry. Representative dot plots and cumulative data from 2 independent experiments (n=2-3 mice per group) are shown (mean + SEM). (**B**) Spleens of 6-week-old WT and cKO mice were analyzed by flow cytometry. Cumulative data from 2 independent experiments (n=2-3 mice per group) are shown. Distribution of naïve, effector memory (EM), and central memory (CM) cells are shown as mean + SEM. (**C**) Absolute cell numbers of T cell subsets are shown. Each symbol represents a mouse.

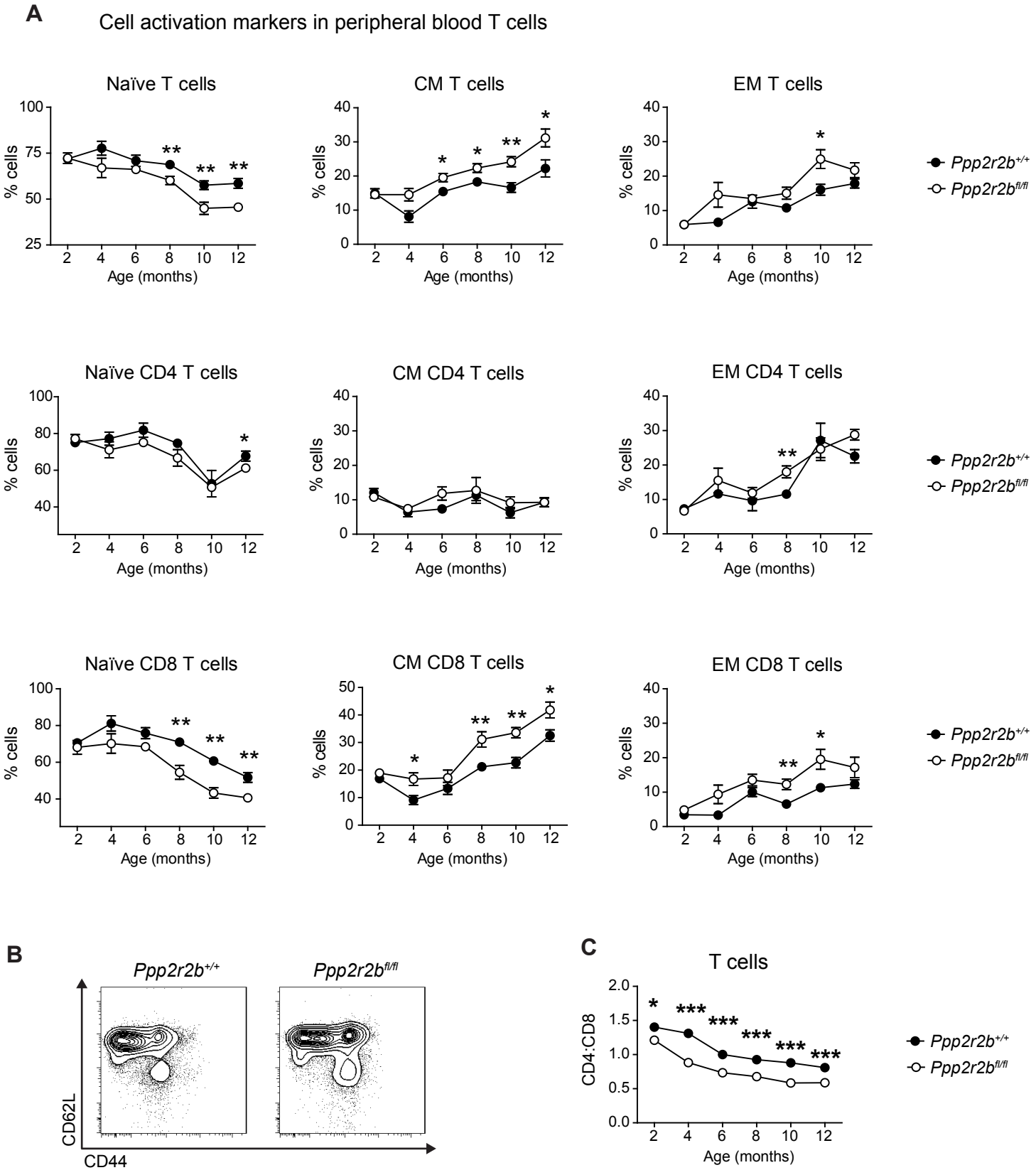

Supplemental Figure 2. T cell-specific B55β deficiency causes gradual accumulation of central memory CD8 T cells. (**A**) The frequency of CD4 and CD8 T cells and their expression of CD44 and CD62L was analyzed by flow cytometry in peripheral blood of wild-type (WT; *Ppp2r2b*$^{+/+}$*Cd4*.Cre^{+}) and conditional knockout (cKO; *Ppp2r2b*$^{fl/fl}$*Cd4*.Cre^{+}) mice every 2 months. Cumulative data from 2 experiments (n=5 mice per group) is shown (mean ± SEM). (**B**) Representative contour plots showing CD44 and CD62L expression on CD3^{+} T cells from 8-month-old WT and a cKO mice. (**C**) CD4:CD8 T cell ratio in peripheral blood of WT and cKO mice. Cumulative data from 1 (out of 2) representative experiments (n=5 mice per group) is shown (mean ± SEM). Unpaired t test was used, * p≤0.05, ** p≤0.01, *** p≤0.001.

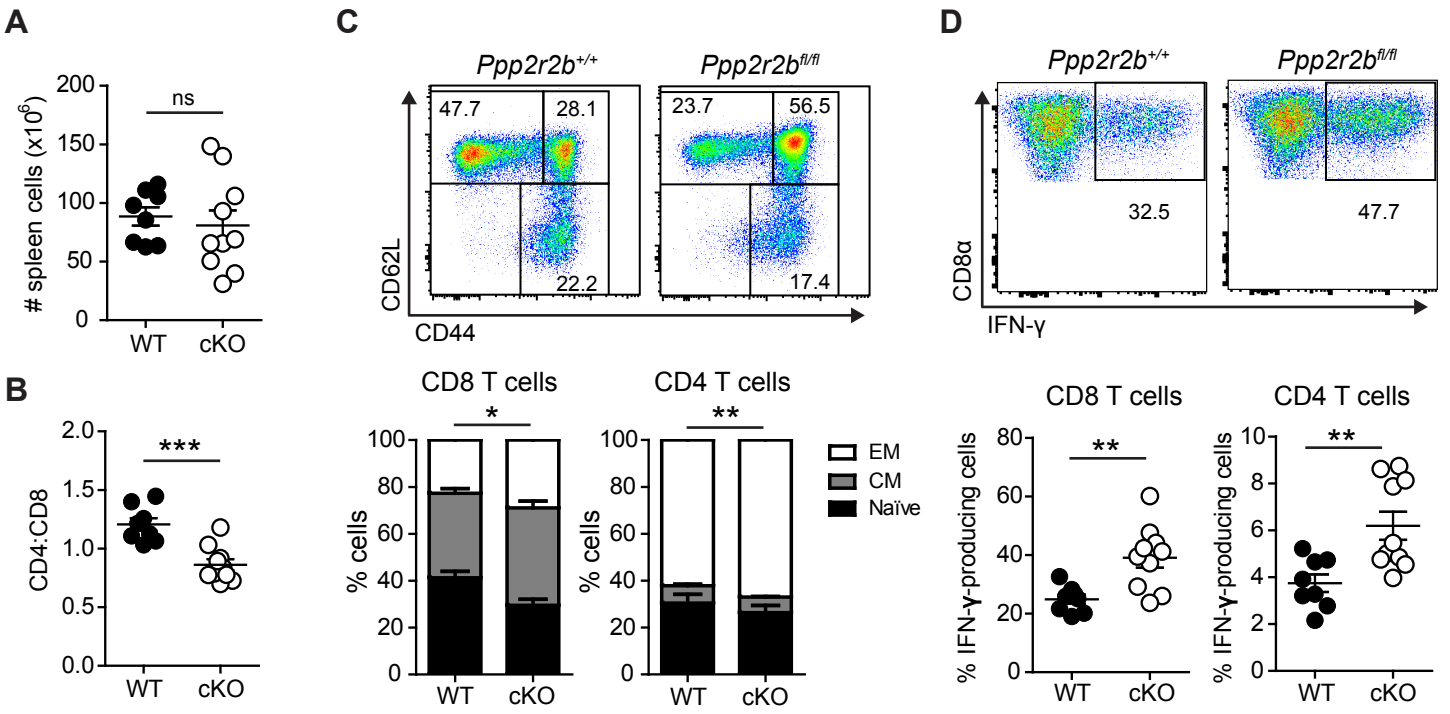

Supplemental Figure 3. T cell-specific B55β deficiency causes accumulation of activated T cells in aged mice. Spleens from 16 month-old wild-type (WT; *Ppp2r2b*$^{+/+}$*Cd4*.Cre^{+}) and conditional knockout (cKO; *Ppp2r2b*$^{fl/fl}$*Cd4*.Cre^{+}) mice were analyzed. (**A**) Absolute cell number and (**B**) CD4:CD8 T cell ratio in spleens from WT and cKO mice. (**C**) Representative dot plots (for CD8 T cells) and cumulative data, depicting the proportion of naïve, central memory (CM), and effector memory (EM) CD8 and CD4 T cells, based on the expression of CD44 and CD62L (CD62L^{+}CD44^{-}, CD62L^{+}CD44^{+}, and CD62L^{-}CD44^{+}, respectively). (**D**) Representative dot plots (for CD8 T cells) and cumulative data indicating the proportion of IFN-γ^{+} CD8 and CD4 lymphocytes from WT and cKO aged mice upon ex vivo overnight stimulation with plate-bound anti-CD3 and anti-CD28. A, B and D, Student's t test; C, two-way ANOVA with Bonferroni's posttest. Cumulative data from 2 experiments (WT, n=8; cKO, n=10) is shown (mean ± SEM). *p≤0.05; **p≤0.01; ***p≤0.001; ns: not significant

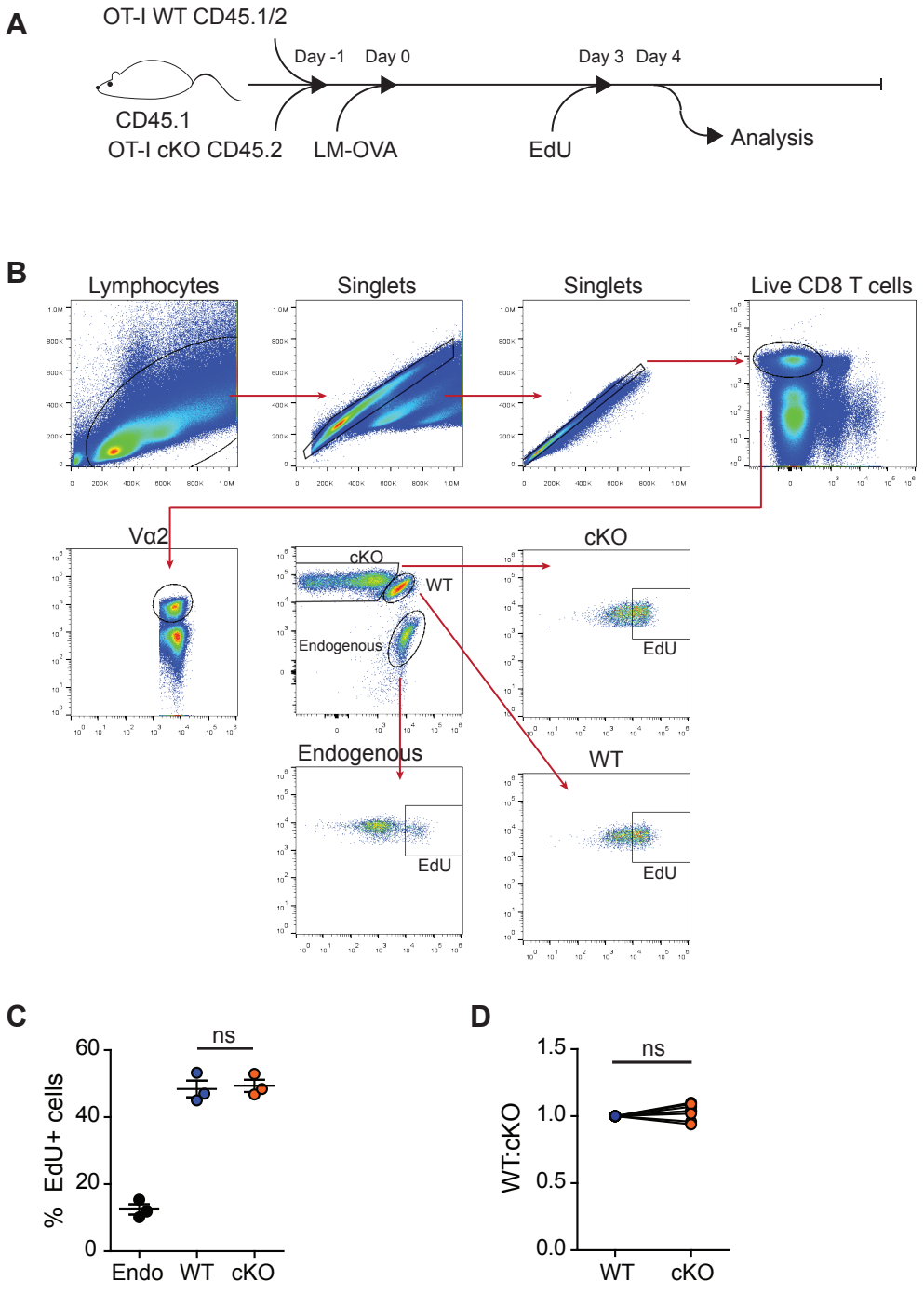

Supplemental Figure 4. B55β deficiency does not affect OT-I cell proliferation during infection with *Listeria monocytogenes*. (**A**) *Ppp2r2b*$^{+/+}$ *Cd4*^{CRE} OT-I CD45.1/2 (WT) cells and *Ppp2r2b*$^{fl/fl}$ *Cd4*^{CRE} OT-I CD45.2 (cKO) cells were adoptively transferred (1:1 ratio) into WT CD45.1 mice. Next day, recipient mice were infected with ovalbumin-expressing *Listeria monocytogenes* (LM-OVA). At day 3 after infection, mice received EdU and were sacrificed 24 hours later to quantify EdU incorporation in cycling WT and cKO OT-I cells. (**B**). Gating strategy used to quantify the relative abundance of WT and cKO cells and to assess EdU incorporation. (**C**) Number of EdU^{+} cells within endogenous (CD45.1) Vα2^{+} cells, and within transferred WT and cKO mice. (**D**) Ratio of WT to cKO cells in the spleens of mice at day 4 after LM-OVA injection. Cumulative data of 3 independent experiments (*n*=1) is shown (**C**-**D**).

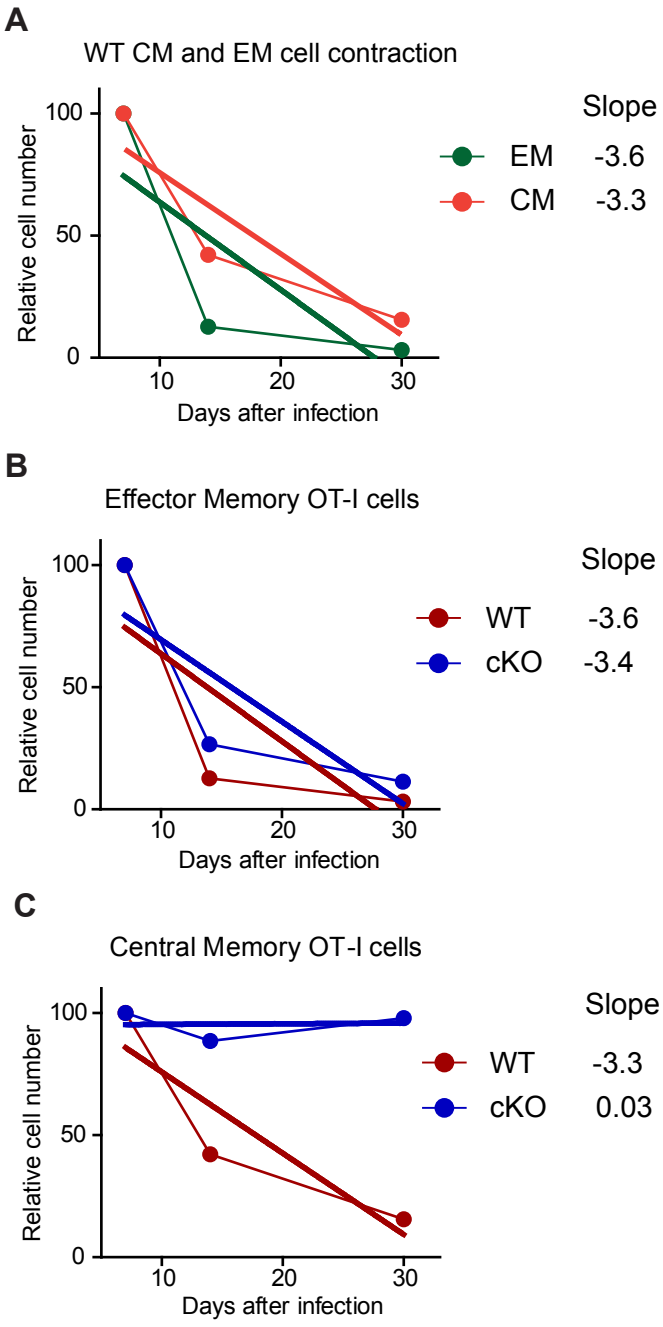

Supplemental Figure 5. Contraction of effector and central memory OT-I T cells in LM-OVA infected mice. (**A**) Relative numbers of effector memory (EM; $CD44^+$ $CD62L^-$) and central memory (CM; $CD44^+$ $CD62L^+$) OT-I cells in mice infected with LM-OVA at the indicated time points. The number of cells at day 7 was considered 100. Non-linear fit of each curve (heavy lines) and its corresponding slope are shown. (**B**) Relative numbers of wild-type (WT; *Ppp2r2b*$^{+/+}$*Cd4*.Cre$^+$) and conditional knockout (cKO; *Ppp2r2b*$^{fl/fl}$*Cd4*.Cre$^+$) EM cells in infected mice. (C) Relative numbers of WT and cKO CM T cells. Cumulative data from one (out of 2) representative experiment is shown (n=3-5 mice per group per time point).

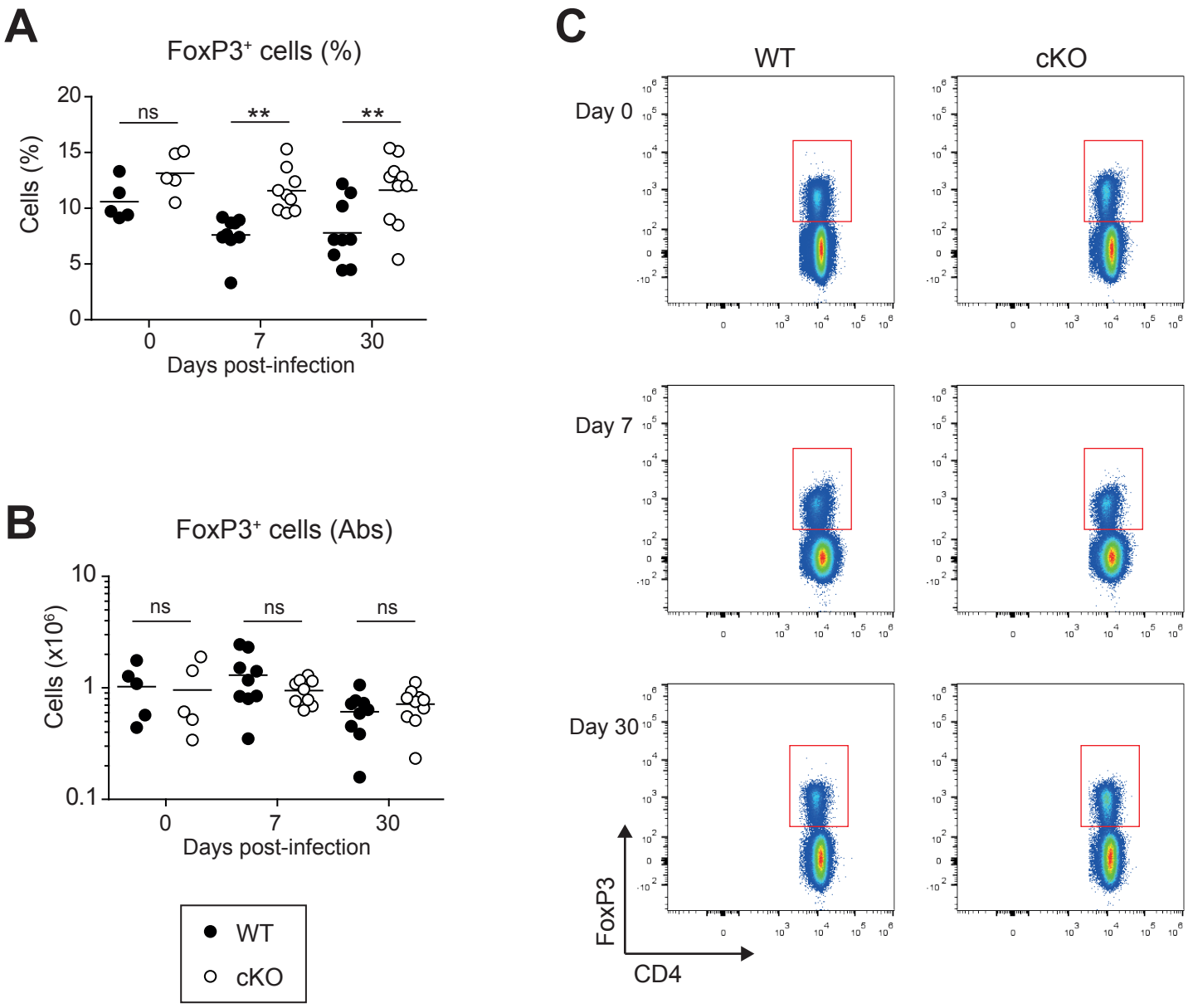

Supplemental Figure 6. *Ppp2r2b* deficiency is associated with a modest increase in the frequency of FoxP3⁺ regulatory T cells during LM-OVA infection. WT (*Ppp2r2b*$^{+/+}$*Cd4*^{CRE}) and cKO (*Ppp2r2b*$^{fl/fl}$*Cd4*^{CRE}) mice were infected with LM-OVA. Before infection (Day 0), as well as 7 and 30 days post-infection, CD4⁺ FoxP3⁺ regulatory T cells were quantified by flow cytometry in spleens. Results are expressed as % of FoxP3⁺ cells within CD4⁺ T cells (**A**), or as absolute CD3⁺ CD4⁺ FoxP3⁺ cells per spleen (**B**). Representative pseudocolor dot plots are shown in (**C**). Cells in (**C**) were pregated as: lymphoid cells (FSC/SSC), singlets, ghost dye⁻ (live) CD3⁺, CD4⁺. Red gate indicates FoxP3⁺ cells. Cumulative data of 2 experiments (*n* = 3-6 mice per group per time point) are shown in **A** and **B**. ** *P*<0.01 (Two-way ANOVA with Bonferroni's posttest).

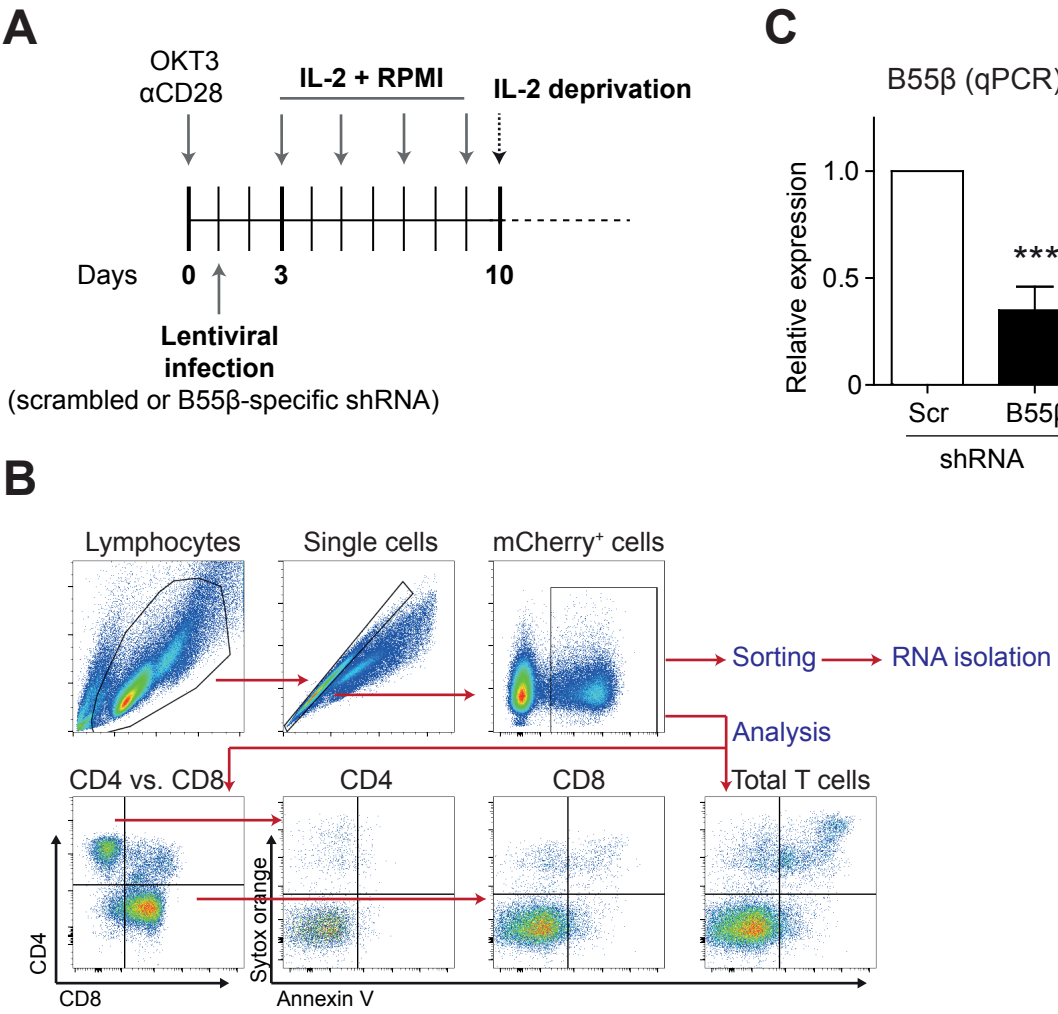

Supplemental Figure 7. B55β silencing in human T cells. (**A**) Purified human T cells were activated with plate-bound anti-CD3 (OKT3, 5 μg/mL) and anti-CD28 (Clone 9.3, 5 μg/mL). Next day, control (scrambled shRNA) or B55β-specific shRNA encoding lentiviruses were added to the culture. During the 10 day expansion period, IL-2 (100 U/mL) and full RPMI were replenished every 48 hours. At day 10, cells were washed and resuspended in fresh RPMI devoid of IL-2. (**B**) Gating strategy used to sort mCherry⁺ cells, or to analyze total T cells, CD4⁺ T cells, and CD8⁺ T cells. (**C**) Knock-down efficiency was analyzed by qPCR in mCherry+ cells 24 hours after IL-2 withdrawal. Cumulative data of 2 independent experiments (*n*=4) is shown as relative expression (ΔΔCt, Mean + SEM). Two-tailed paired Student's t test was used. *** p=0.001.

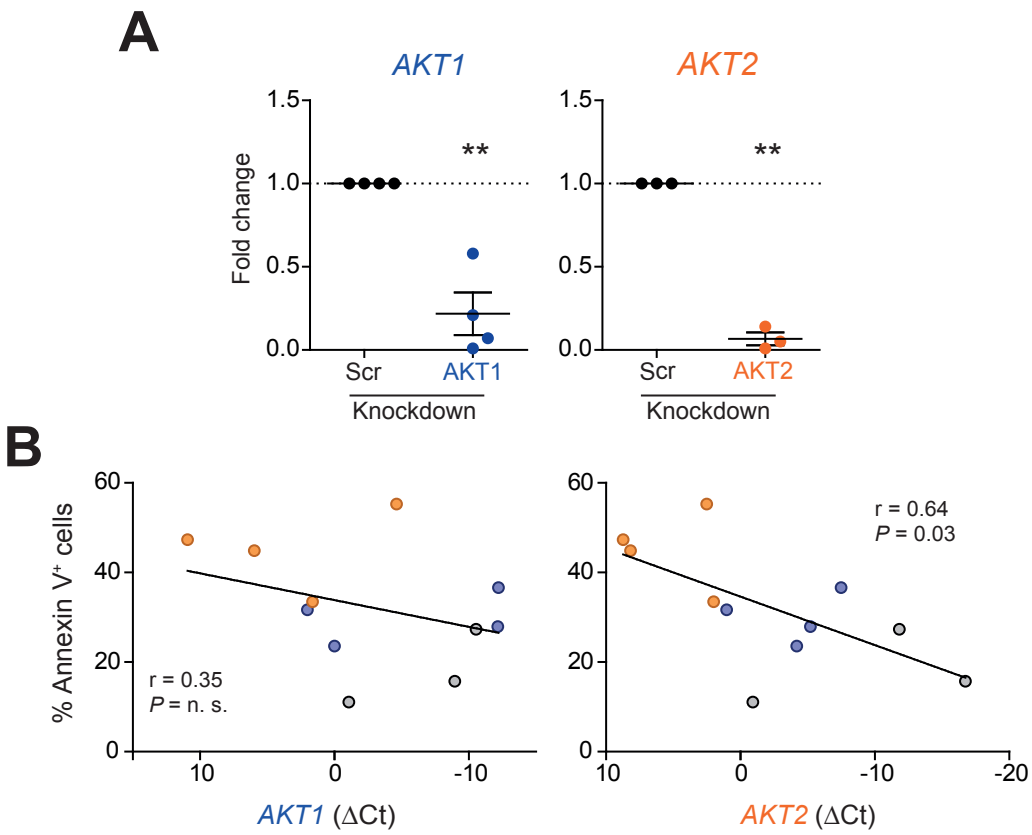

Supplemental Figure 8. AKT2 represents the predominant AKT isoform during cytokine withdrawal. (**A**) Lentiviruses encoding shRNA specific for *AKT1* or *AKT2* (or scrambled; Scr) were used to knockdown the corresponding genes. *AKT1* and *AKT2* levels are shown as fold change over cells infected with control viruses. ** $P<0.001$ (two-tailed paired Student's t test). (**B**) The data from Figure 4E was used to determine whether a correlation exists between *AKT1* (left) and *AKT2* (right) levels (shown as ΔCt) and apoptosis. Pearson r and two-tailed P values are shown. Cumulative data from 3 experiments (n = 1-3) is shown (**A-D**).

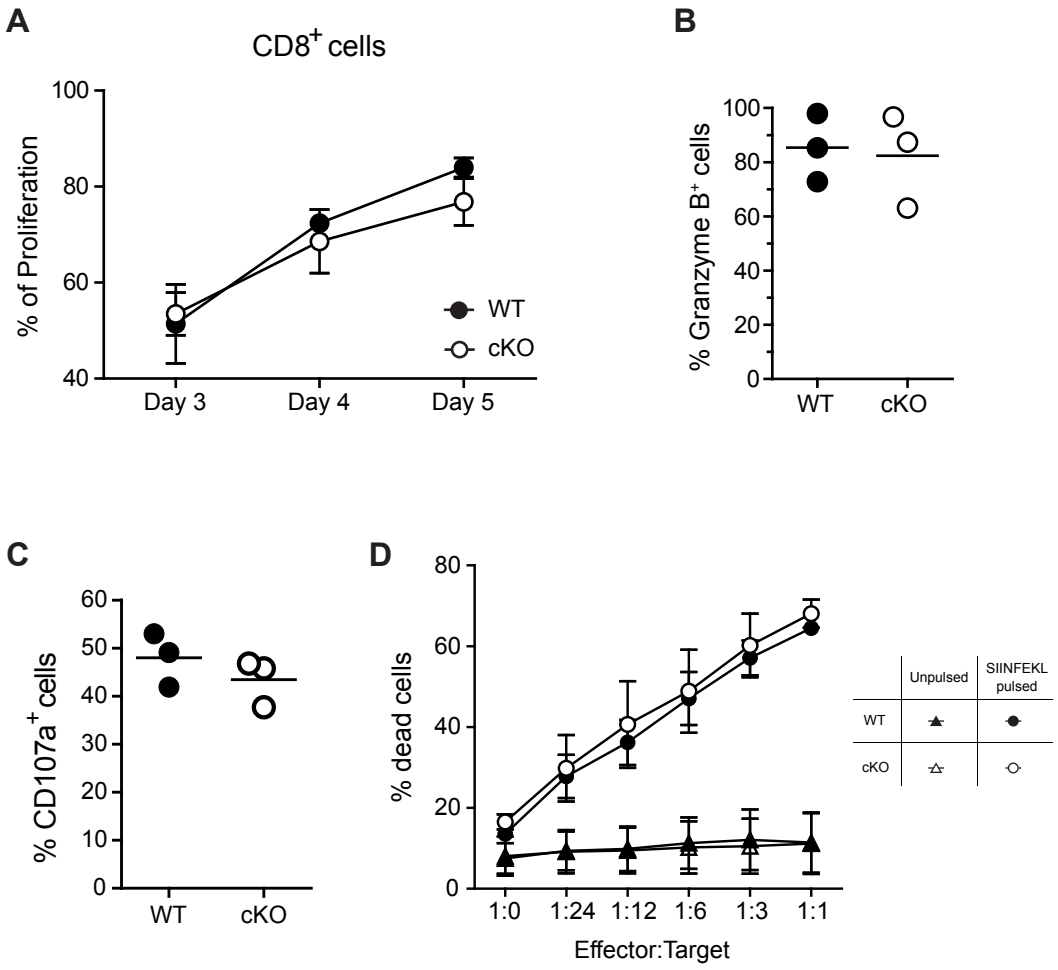

Supplemental Figure 9. B55β deficiency does not affect CD8 T cell proliferation or effector capacity (**A**) T cells from WT (*Ppp2r2b*$^{+/+}$*Cd4*.Cre^{+}) or cKO (*Ppp2r2b*$^{fl/fl}$*Cd4*.Cre^{+}) mice were CFSE-labeled and activated with plate-bound anti-CD3 (2 μg/mL) and anti-CD28 (2 μg/mL). CFSE^{lo} cells were quantified at the indicated time points. (**B**) Proportion of granzyme B-producing CTLs from WT or cKO mice after incubation (16-24 hours) with SIINFEKL-pulsed spleen cells. (**C**) Degranulation efficiency (measured as CD107a^{+} cells) of CTLs from WT and cKO mice after 5 hours in contact with SIINFEKL-pulsed spleen cells. (**D**) Cytotoxic activity of WT and cKO CTLs incubated for 5 hours with unpulsed (triangles) or SIINFEKL-pulsed (circles) target spleen cells. (**A**-**D**) Cumulative data from 3 experiments are shown (n=1-3 mice per group). No significant differences (Student´s t test or ANOVA) were found. Results are expressed as mean ± SEM.

Supplemental Table 1. Plasmids and backbones

Plasmid	Source	Investigator	Reference
LeGO-C	Addgene (#27348)	Boris Fehse	(Weber et al., 2008)
LeGO-G	Addgene (#27347)	Boris Fehse	(Weber et al., 2008)
LeGO-Cer	Addgene (#27351)	Boris Fehse	(Weber et al., 2008)
pWPI	Addgene (#12254)	Didier Trono	N.A.
pLVX-IRES-mCherry	Clontech (631237)	N.A.	N.A.
GFP-Foxo1	Addgene (#17551)	Domenico Accili	(Frescas et al., 2005)
psPAX2	Addgene (#12260)	Didier Trono	N.A.
pMD2.G	Addgene (#12259)	Didier Trono	N.A.

Abbreviation: N.A., not available

Supplemental Table 2. Antibodies

Antibody	Clone/Cat No.	Source
mCD3-PB	17A2	Tonbo Biosciences
mCD4-FITC/APC-Cy7	RM4-5	Biolegend
mCD8-FITC/PE	53-6.7	Biolegend
mCD62L-APC/redFluor710	MEL-14	Biolegend
mCD44-APC-Cy7	IM7	Biolegend
mCD25-APC	PC61	Biolegend
mFoxP3-PE	150D	Biolegend
mCD45.1-FITC/BV605/APC-Cy7	A20	Biolegend
mCD45.2-redFluor710/APC-Cy7	104	Tonbo Biosciences
mTCR-Vα2-FITC/PE	B20.1	Biolegend
mTCR-Vβ5-PE-Cy7	MR9-4	Biolegend
mKLRG1-violetFluor450	2F1	Tonbo Biosciences
mCD127-PE-Cy7	A7R34	Tonbo Biosciences
mIFN-γ-APC/PE-Cy7	XMG1.2	Tonbo Biosciences
mGranzyme B-eFluor 450	NGZB	eBiosciente
mCD107a (LAMP-1)-PE	1D4B	Biolegend
hCD3 PB/APC-Cy7	OKT3	Tonbo Biosciences
hCD4-FITC/PerCP5.5	OKT4	Tonbo Biosciences
hCD8a-APC-Cy7/PerCP5.5	RPA-T8	Tonbo Biosciences
mCD3	145-2C11	BioXCell
mCD28	37.51	BioXCell
hCD3	OKT3	BioXCell
hCD28	9.3	BioXCell
AKT	40D4	Cell Signaling Technology
pAKT S473	D9E	Cell Signaling Technology
pAKT-S473-Alexa Fluor 488	D9E	Cell Signaling Technology
pAKT T308	C31E5E	Cell Signaling Technology
β-actin	AC-15	Sigma Aldrich
Goat anti-mouse	Cat No: 32230	Pierce
Goat anti-rabbit	Cat No: 32260	Pierce

Abbreviations: m, mouse; h, human; PB, pacific blue; APC, allophycocyanin; APCy7, APC-Cyanine 7; PE, phycoerythrin; PerCP5.5, peridinin chlorophyll-A protein 5.5; PE-Cy7, PE-Cyanine 7.

Supplemental Table 3. Key Reagents

Reagent	Identifier	Source
mIL-2	Clone: JES6-1A12	BioXCell
hIL-2	Clone: MQ1-17H12	Biolegend
rhIL-2	Cat No: 200-02	Peprotech
rhIL-7	Cat No: 200-07	PeproTech
rhIL-15	Cat No: 200-15	PeproTech
Annexin V-FITC	Cat No: 640945	Biolegend
Annexin V-APC	Cat No: 640941	Biolegend
Sytox Orange	Cat No: S11368	Thermo Fisher
Ghost Dye Red 780	Cat No: 13-0865-T500	Tonbo
CellTrace Far Red	Cat No: C34564	Thermo Fisher
FAM-FLICA Caspase-3/7 Assay Kit	Cat No: 94	ImmunoChemistry
Lipofectamine 2000	Cat No: 12566014	Thermo Fisher
BD GolgiPlug (Brefeldin A)	Cat No: 555029	BD Biosciences
Monesin	Cat No: 420701	Biolegend
Phorbol 12-myristate 13-acetate (PMA)	Cat No: P8139	Sigma
Ionomycin	Cat No: I0634	Sigma
Annexin V binding buffer	Cat No: 422201	Biolegend
Polybrene	Cat No: H9268	Sigma-Aldrich
Pierce ECL Western blotting substrate	Cat No: QK222185A	Thermo Fisher
SIINFEKL	Cat No: RP10611	GenScript
Hoechst 33342	Cat No: 62249	Thermo Fisher
Chloramphenicol	Cat No: C0378	Sigma

Brain Heart Infusion (BHI)	Cat No: 237300	BD Bacto
TRIzol	Cat No: 15596018	Thermo Fisher
PathScan Akt signaling antibody array kit	Cat No: 9474	Cell Signaling Technology
CD8α^+ T Cell Isolation Kit II	Cat No: 130-095-236	Miltenyi Biotec
BD Cytofix/Cytoperm	Cat No: 554714	BD Biosciences
Dynabeads Untouched Human T Cells Kit	Cat No: 11344D	Thermo Fisher
SCRIPT Reverse Transcriptase	Cat No: PCR-505	Jena Bioscience
Click-iT Plus EdU Pacific Blue Kit	Cat No: C10636	Thermo Fisher
Fetal Bovine Serum	Cat No:11560636	Gibco
Roswell Park Memorial Institute 1640 Medium	Cat No: 11875135	Sigma-Aldrich
Dulbecco´s Modified Eagles´s Medium	Cat No. D5030	Sigma-Aldrich
FoxP3/Transcription Factor Staining Buffer Set	Cat No: 00-5523-00	Thermo Fisher
Trypsin solution	Cat No: 59427C	Sigma-Aldrich
LY-294002	Cat No: PHZ1144	Thermo Fisher
MK-2206	Cat No: 1031320	PeproTech
Rapamycin	Cat No:5318893	PeproTech
FR180204	Cat No: SML0320	Sigma-Aldrich
PD98059	Cat No: P215	Sigma-Aldrich
SB202190	Cat No: S7067	Sigma-Aldrich

Supplemental Table 4. shRNA sequences

Oligo	Sequence
h*PPP2R2B*_1	F: TGACCTGAGGATTAACCTATTTCAAGAGAATAGGTTAATCCTCAGGTCTTTTTTC R: TCGAGAAAAAAGACCTGAGGATTAACCTATTCTCTTGAAATAGGTTAATCCTCAGGTCA
h*PPP2R2B*_2	F: TGTGGAATGGGTCAGACAGTTTCAAGAGAACTGTCTGACCCATTCCACTTTTTTC R: TCGAGAAAAAAGTGGAATGGGTCAGACAGTTCTCTTGAAACTGTCTGACCCATTCCACA
m*Hrk*_1	F: TCCAGTGCTATTTAGCTATATATTCAAGAGATATATAGCTAAATAGCACTGGTTTTTTC R:TCGAGAAAAAAACCAGTGCTATTTAGCTATATATCTCTTGAATATATAGCTAAATAGCACTGGA
m*Hrk*_2	F: TGTAATGGAAACCACGTATTTATTCAAGAGATAAATACGTGGTTTCCATTACTTTTTTC R:TCGAGAAAAAAGTAATGGAAACCACGTATTTATCTCTTGAATAAATACGTGGTTTCCATTACA
h*AKT1*	F: TGCACTTTCGGCAAGGTGATTTCAAGAGAATCACCTTGCCGAAAGTGCTTTTTTC R: TCGAGAAAAAAGCACTTTCGGCAAGGTGATTCTCTTGAAATCACCTTGCCGAAAGTGCA
h*AKT2*	F: TGGCTAAAGTGACCATGAATTTCAAGAGAATTCATGGTCACTTTAGCCTTTTTTC R: TCGAGAAAAAAGGCTAAAGTGACCATGAATTCTCTTGAAATTCATGGTCACTTTAGCCA

Abbreviations: m, mouse; h, human; F, forward; R, reverse.

Supplemental Table 5. Real-time PCR primers

Gene	Forward	Reverse
Human_*HRK*	TACTGGCCTTGGCTGTGC	CACAGGGTTTTCACCAACCT
Human_*BCL2L11*	CATCGCGGTATTCGGTTC	TTGCTTTGCCATTTGGTCTT
Human_*PMAIP1*	GTCCTCAGCCCTCGCTCT	CTAATTGGGCTCCATCTCG
Human_*BBC3*	GGAGATGCCTGGGAAGAAG	CCTGAGTTGAGTAGCACACTCG
Human_*ACTB*	CCACCATCACGCCCTGG	ATGATGATATCGCCGCGCTC
Human_*PPP2R2B*	ATCCTGCCACCATCACAAC	GCGTTGGCAAATACTCTTCG
Human_*BCL2*	ATCTTTATTTCATGAGGCACGT	TTGACAGAGGATCATGCTGTACT
Human_*BCL2L1*	GGGAGGGTAGAGTGGATGGT	GCTTGGATGGCCACTTACCT
Human_*AKT1*	GGCTATTGTGAAGGAGGGTTG	TCCTTGTAGCCAATGAAGGTG
Human_*AKT2*	GCTCCACAAGCGTGGTGAAT	TGTACCCAATGAAGGAGCCG
Human_*AKT3*	TTGCTTTCAGGGCTCTTGAT	CATAATTTCTTTTGCATCATCTGG
Mouse_*Pmaip1*	TTCTCCGGAGTGTTCATGC	TACAGCGGAGGGCATCAG
Mouse_*Hrk*	GGAGAGGGGCAGCAGACTA	GTGATGTCTTAGTGGGGCTTCT
Mouse_*Bcl2l11*	GGAGACGAGTTCAACGAAACTT	GTGATGTCTTAGTGGGGCTTCT
Mouse_*Bbc3*	CAGATGCCTGGGAAGTCG	TGAGCACACTCGTCCTTCAA
Mouse_*Actb*	GCAGGAGTACGATGAGTCCG	ACGCAGCTCAGTAACAGTCC
Mouse_*Bcl2l1*	TGACCACCTAGAGCCTTGGA	AAGAGTGAGCCCAGCAGAA
Mouse_*Bcl2*	AGTACCTGAACCGGCATCTG	GGGGCCATATAGTTCCACAAA

Supplemental References

Frescas, D., Valenti, L., and Accili, D. (2005). Nuclear trapping of the forkhead transcription factor FoxO1 via sirt-dependent deacetylation promotes expression of glucogenetic genes. J. Biol. Chem. *280*, 20589–20595.

Weber, K., Bartsch, U., Stocking, C., and Fehse, B. (2008). A Multicolor Panel of Novel Lentiviral “Gene Ontology” (LeGO) Vectors for Functional Gene Analysis. Mol. Ther. *16*, 698–706.